Electronic Supplementary Material (ESI) for Journal of Materials Chemistry C.
This journal is © The Royal Society of Chemistry 2020

Supporting Information

Intrinsically healing artificial neuromorphic device

Yujie Yan,[a,b] Xiaomin Wu, [a] Qizhen Chen, [a] Xiumei Wang, [a] Enlong Li, [a] Yuan Liu,[c] Huipeng Chen, [a,b]*Tailiang Guo[a,b]

[a] *Institute of Optoelectronic Display, National & Local United Engineering Lab of Flat Panel Display Technology, Fuzhou University, Fuzhou 350002, China*

[b]*Fujian Science & Technology Innovation Laboratory for Optoelectronic Information of China, Fuzhou 350100, China*

[c] *State Key Laboratory for Chemo/Biosensing and Chemometrics, School of Physics and Electronics, Hunan University, Changsha 410082, China*

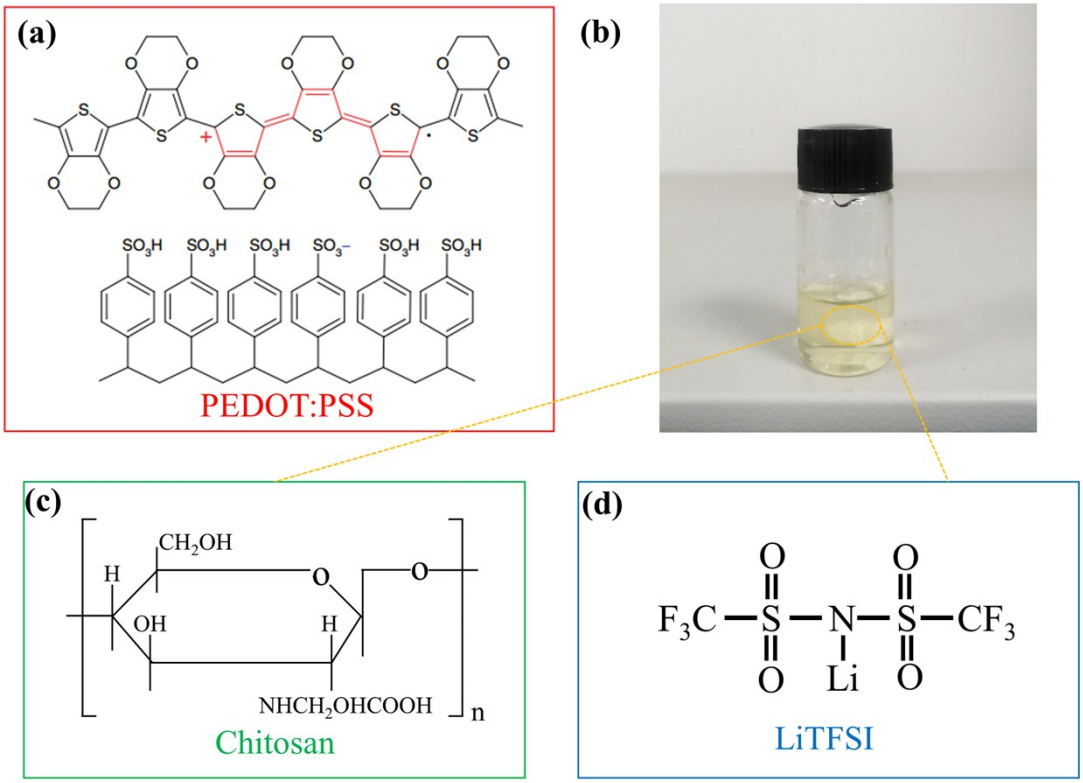

Fig. S1 Chemical structure of healable components. The chemical structure of (a) PEDOT:PSS, (c) chitosan and (d) LiTFSI, respectively. (b) The photographic image of ionic hydrogel.

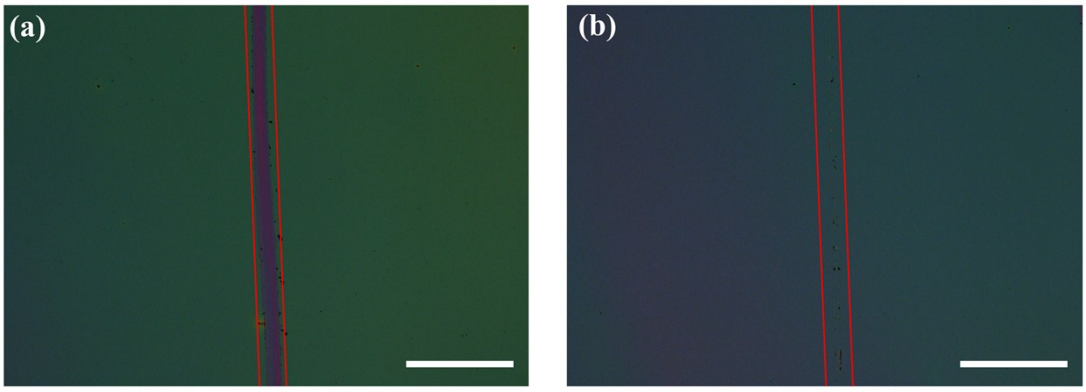

Fig. S2 Healability of hydrogel films. The optical images of individual hydrogel films (a) before and (b) after healing by water. Scare bar: 200 μm. The hydrogel film exhibited high healing ability as well.

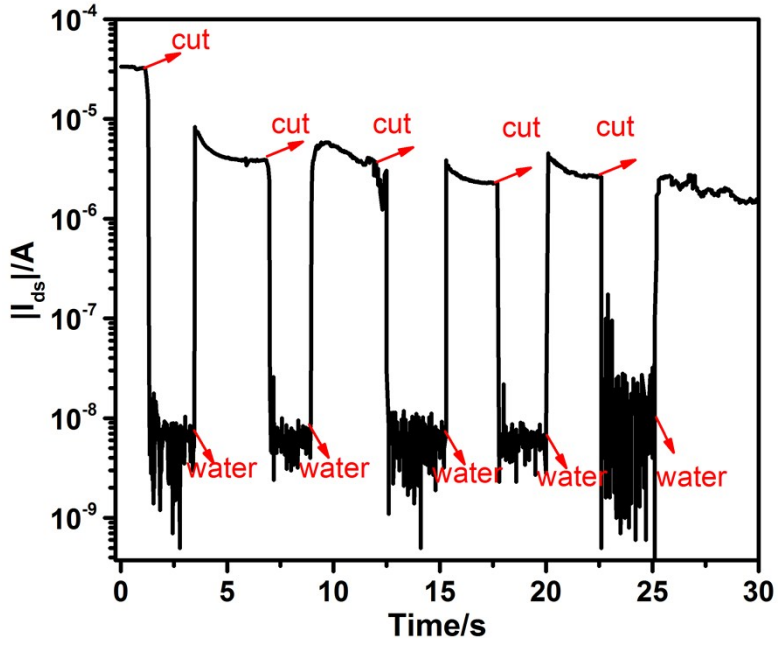

Fig. S3 Testing stability of damage-healed cycles. Current versus time measurements (applied voltage 1 V) for PEDOT:PSS/hydrogel film showing the effect of damage and healing triggered by water. The damage/healing process was repeated five times on different regions of the film, where the recovered current was tended to stabilize after the first time damaged-healed cycle, suggesting that the remarkable reliability and reproducibility of the healing process. As a result, DI water is an efficient and cost-effective healing agent for repairing the PEDOT:PSS/ionic hydrogel films.

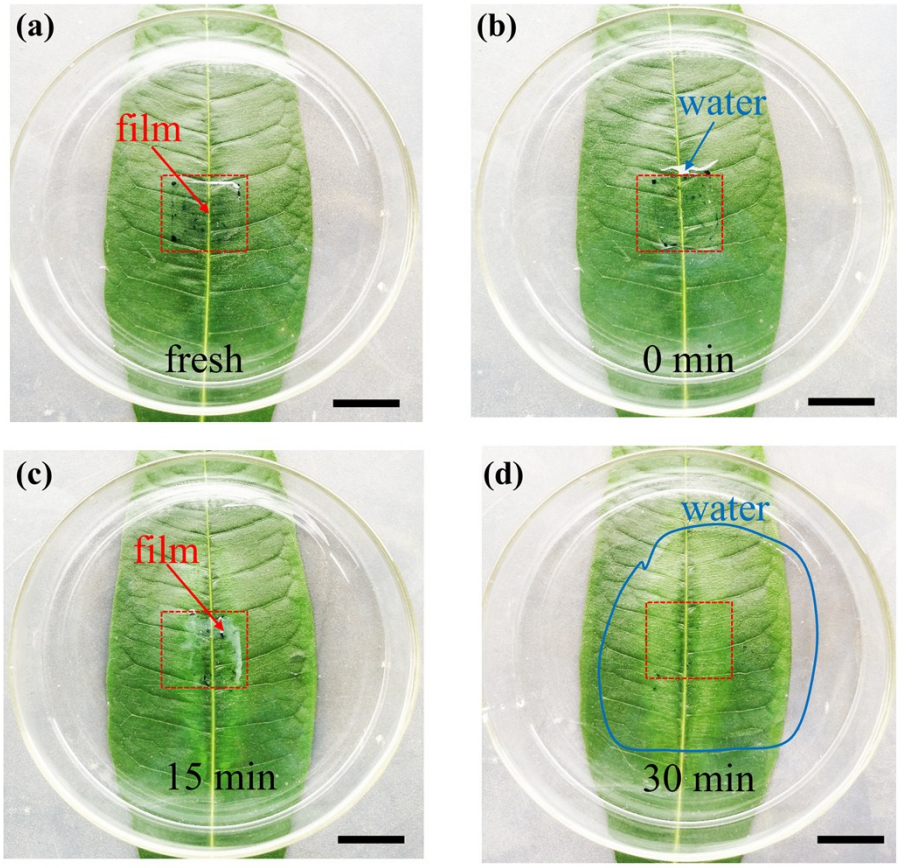

Fig. S4 Biodegradable process of PEDOT:PSS/hydrogel films. The decomposition process of biodegradable PEDOT:PSS/hydrogel film, triggered by the treatment of DI water. (a) fresh, (b) 0 min, (c) 15 min, (d) 30 min. Scale bar: 1 cm. The PEDOT:PSS/hydrogel films were found to have biodegradability triggered by DI water, which was a crucial biomimetic property.

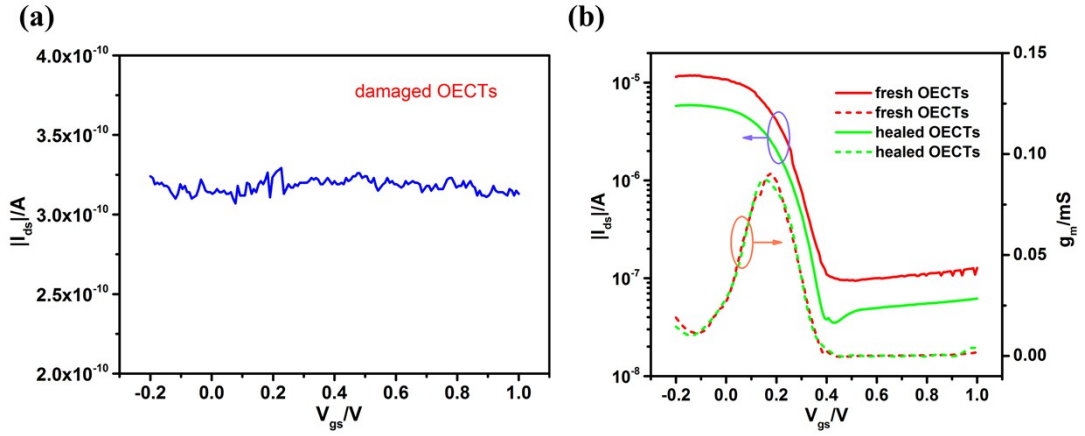

Fig. S5 The transfer characteristic of healing organic electrochemical transistors (OECTs) based on healable PEDOT:PSS and hydrogel (a) before and (b) after healing.

As shown in Figure S5a, the output current (I_{ds}) in damaged OECTs could not be controlled by gate voltage and its value was approximately 10^{-10} A, indicating the completely cracked channel. On the contrary, as shown in Figure S5b, the healed devices exhibited a representative depletion-type electrolyte-gated transistor property, which suggested that the damaged channel and ionic hydrogel were both well healed.

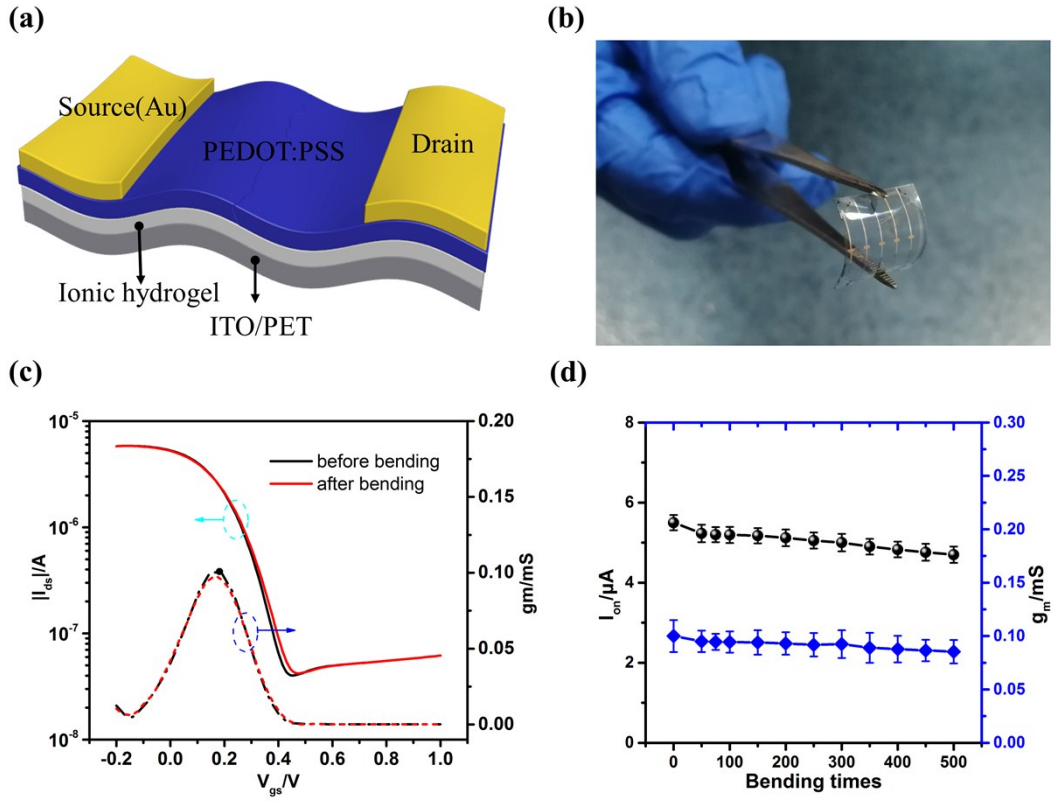

Fig. S6 Device performance of flexible healing synaptic device at bending states. (a) Schematic diagram and (b) photographic images of flexible OECTs. (c) The transfer and transconductance (g_m) characteristics for the flexible before and after bending at bending radius of 18 mm. (d) Cycle stability of peak transconductance and on-current of flexible devices as a function of bending times at bending radius of 10 mm. As shown in Figure S6c, The transfer and transconductance characteristics of the flexible devices before bending were similar to that of device when bending, exhibiting excellent mechanical flexibility. To gain more insight, the endurance characteristic of flexible devices was investigated in terms of bending times from 50 to 500 times. As shown in Figure S6d, the peak transconductance and on-state current of the flexible uOECTs were observed to be slightly decreased after 500 bending times, which was due to not only the inherent flexibility of organic materials, but also its volumetric

charge transport in the channel that was less affected by the interfaces and cracks inside the channel under mechanical bending.

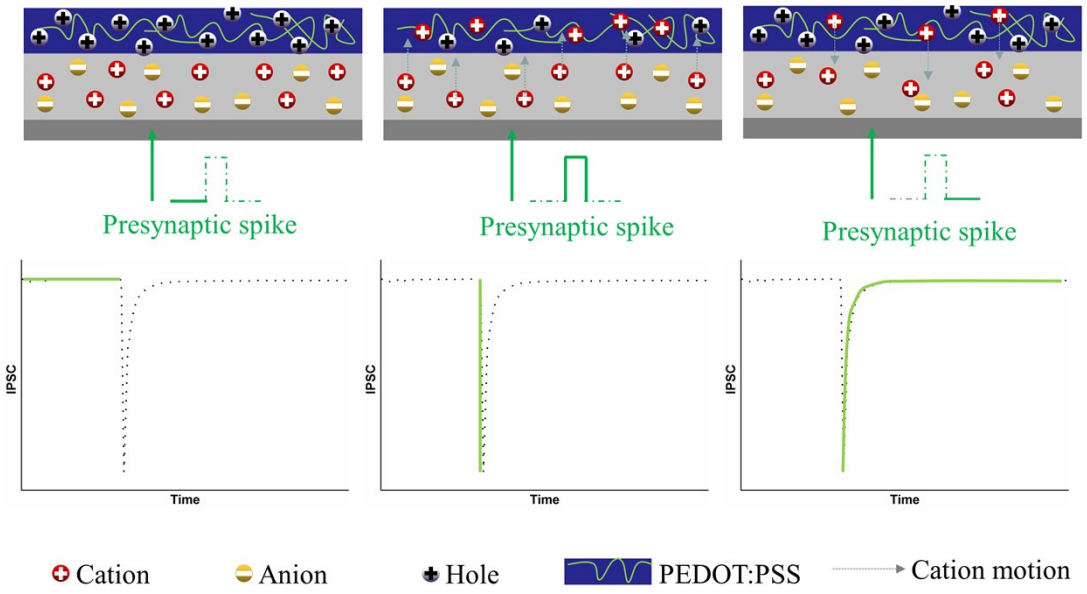

Fig. S7 Schematic of the working mechanism of healable synaptic devices. The top panel is the schematic diagram of hole distribution in the PEDOT:PSS channel and the ion migration dynamics in the ionic hydrogel, and the bottom panel is the triggered postsynaptic current before, during and after the presynaptic spike.

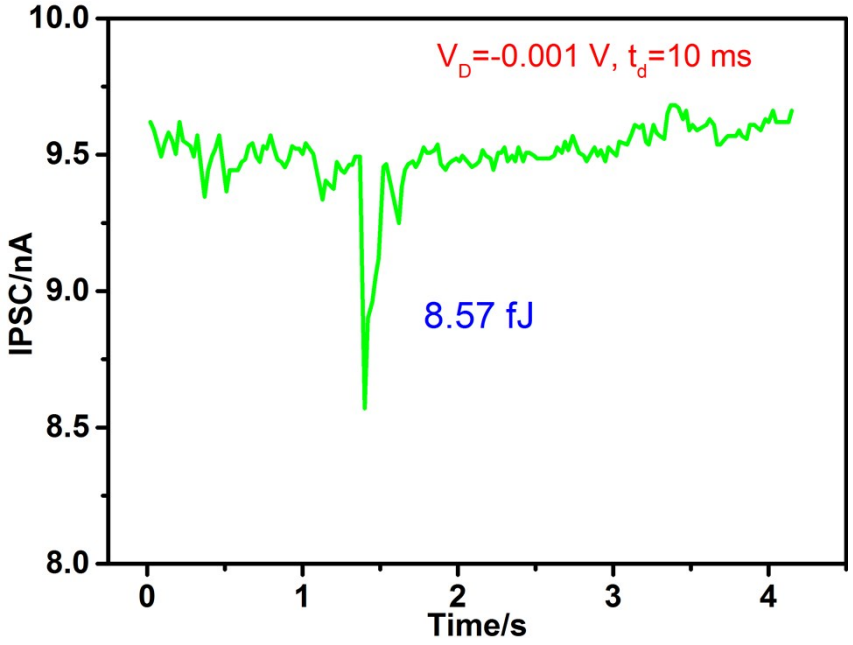

Fig. S8 Energy consumption per spike for inhibitory postsynaptic current (IPSC) triggered by a presynaptic spike with V_{pre}= 0.3 V, t_d= 10 ms and V_{ds}= -0.001 V. Energy consumption of per spike was estimated using the following equation:

$$W = I_{peak} \times t_d \times V_{ds} \quad \text{(S1)}$$

where I_{peak}, t_d and V_{ds} is the spike peak current, the spike duration time, and the source-drain voltage, respectively. The optimized energy consumption was estimated to be 8.57 fJ, which was competitive with other state-of-the-art synaptic devices.

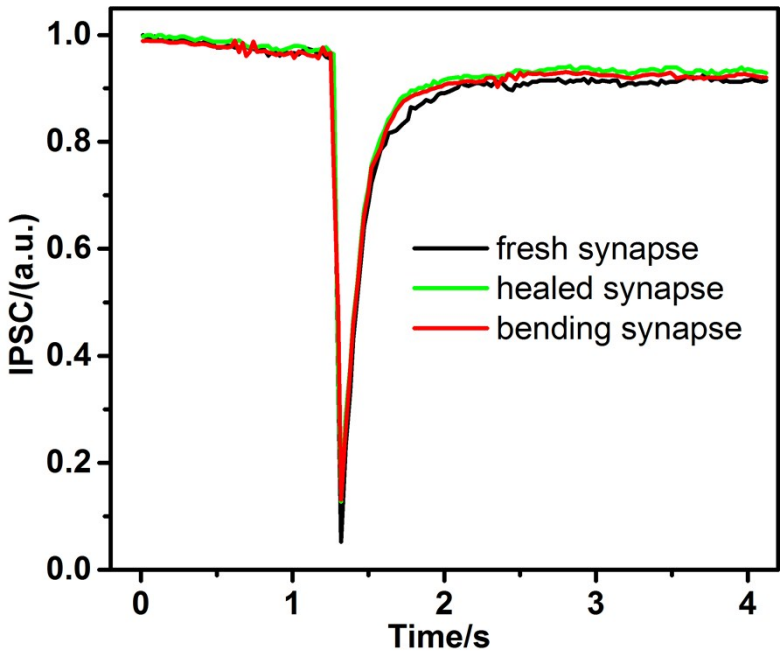

Fig. S9 Comparison of IPSC of fresh, healed, and bending synaptic device. The normalized IPSC of fresh, healed and bending synaptic device triggered by a single spike. The response remained unchanged, and no degradation was observed, when they were healed after damage and bent under a bending radius of 18mm, suggesting fully recovered synaptic functionality and excellent mechanical flexibility.

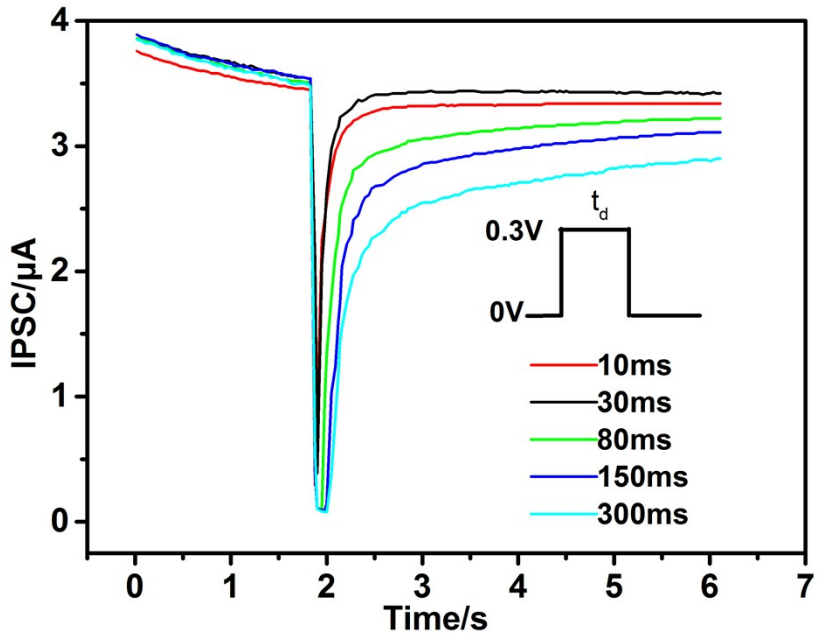

Fig. S10 The IPSC of healed synaptic device triggered by a single spike with same presynaptic spike voltage and different time of duration from 10 to 300 ms. The recovering time of IPSC increased with increasing the duration time of the spike and all IPSC gradually recovered the resting current, indicating a short-term characteristic, which is also agreement with the a short-term characteristic in the biological inhibitory synapse.

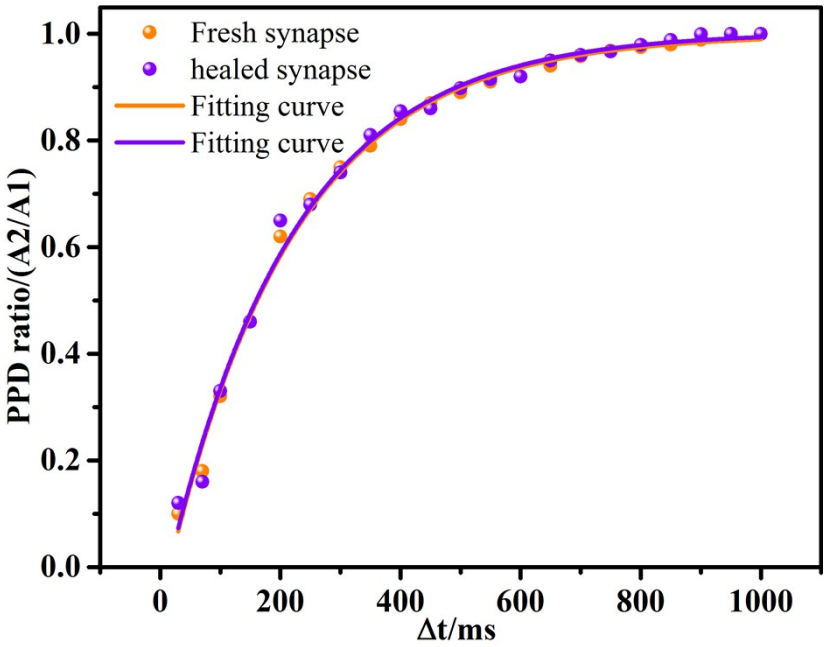

Fig. S11. The paired-pulse depression (PPD) index (*A*2/*A*1) as function of spike interval time (Δt). As Δt increased, the number of residual Li^+ ions in channel triggered by the first spike decreased, resulting in an increase of PPD index. This interval time-dependent depression behavior was well fitted by following a single-exponential function:

$$PPD = c\exp\left(-\frac{\Delta t}{\tau}\right) + I_{\infty} \quad \text{(S2)}$$

Where Δt is the interspike interval, c and τ represent the initial depression magnitudes and the characteristic relaxation times, I_{∞} is the final postsynaptic current. c=100.32 % and τ=210.82 ms were obtained from fitting for healed synaptic devices, which was very similar to the PPD of biological synapse. In addition, the fitted curve of PPD index in the healed synaptic device was the same with that of the fresh synaptic device, suggesting the recovered synaptic functionality after healing.

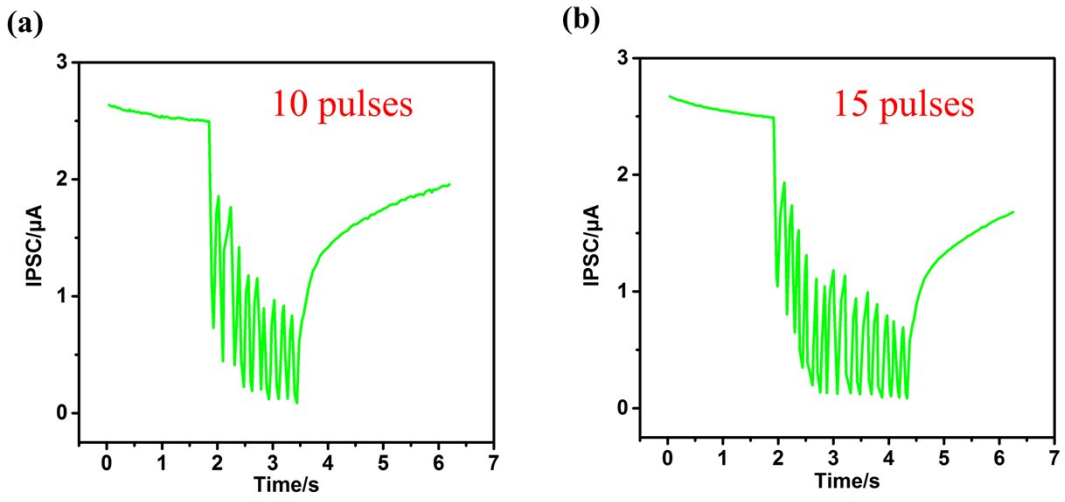

Fig. S12. Adaptation behaviors of synaptic devices. IPSC triggered by a stimulus train of (a) ten and (b) fifteen presynaptic pulses with an interval of 80 ms and duration of 40 ms. With increasing pulse to 10 and 15, the IPSC response exhibited adaptation, as it initially responded to the train of pulses and subsequently adapted to it, which also demonstrated that adaption was a important form of STP in nature.